Holocene Vegetation and Climate Changes in the Huangqihai Lake Region, Inner Mongolia

TIAN Fei[1,*], WANG Yong[1], ZHAO Zhili[1], LI Yang[2], DONG Jin[1], LIU Jin[3], LING Yuan[1], YUAN Lupeng[1] and YE Mengni[1]

[1] *Institute of Geology, Chinese Academy of Geological Sciences, Beijing 100037, China*
[2] *China Solibase Engineering Co., Ltd., Beijing 101300, China*
[3] *School of Civil and Architecture Engineering, Xi'an Technological University, Xi'an 710021, China*

Abstract: A consensus on Holocene climate variability at the modern northern fringe of the East Asian summer monsoon (EASM) region remains elusive. Here, we present a pollen-based reconstruction of vegetation history and associated climate variations of a sediment core from Huangqihai Lake, central Inner Mongolia. During 10.7 to 8.8 cal kaBP, typical steppe with small patches of forest dominated the lake area, suggesting a moderately wet climate, followed by ameliorating climatic conditions until 8.0 cal kaBP as deduced by the expansion of forest. Typical steppe recovered the lake area between 8.0 and 7.2 cal kaBP, reflecting a deterioration of climatic conditions; in combination with other proxy records in the study region, we noticed that severe aridity was prevailed in the lake area between 8.0 and 7.6 cal kaBP. During 7.2 to 3.2 cal kaBP, abundant tree pollen indicated dominance of forest-steppe around the lake, marking regionally wet conditions. A notable absence of broadleaved trees after 5.2 cal kaBP reveals a slight drying trend, and climate deterioration from 4.5 to 4.1 cal kaBP might be linked to the 4.2 ka event. After 3.2 cal kaBP, a transition to steppe was associated with dry conditions in the region. Based on our pollen record and prior paleoclimatic reconstructions in the Huangqihai Lake region, there was a generally-accepted, stepwise shift to a wet climate during the early Holocene, an overall humid climate from 7.2 to 3.2 cal kaBP, and then severe drought for the rest of the Holocene. Moreover, regional comparisons among pollen records derived from lakes situated in the temperate steppe region suggested a roughly synchronous pattern of vegetation and climate changes during the Holocene and demonstrated an intensified EASM during the middle Holocene.

Key words: pollen, paleovegetation, Holocene, East Asian summer monsoon, Huangqihai Lake

Citation: Tian et al., 2020. Holocene Vegetation and Climate Changes in the Huangqihai Lake Region, Inner Mongolia. Acta Geologica Sinica (English Edition), 94(4): 1178–1186. DOI: 10.1111/1755-6724.14565

1 Introduction

Knowledge of Holocene climate variations forms the basis for understanding dynamic mechanisms of the earth system and for predicting future climate change. Lakes located at the modern fringe of the East Asian summer monsoon (EASM) are sensitive to variations in monsoonal precipitation, and their lacustrine sediments have long been used to reconstruct paleoclimate changes and associated EASM intensity (e.g., Wang et al., 2001; Li et al., 2004; Xiao et al., 2006; 2009; 2012; Wang et al., 2013a; Guo et al., 2018). However, regional differences in Holocene climate change, reconstructed from the EASM margin, are still conspicuous due to chronological uncertainties and ambiguities in proxy interpretations, hindering our understanding of EASM evolution (Yang et al., 2018).

The pollen record from Daihai Lake shows mild and dry climatic conditions during the early Holocene (10.25–7.9 cal kaBP) and a warm and humid climate over the subsequent period of 7.9–4.45 cal kaBP (Xiao et al., 2004). It is further demonstrated that the maximum precipitation, indicated by the expansion of mixed pine and broadleaved forests, occurred from 6.05 to 5.1 cal kaBP. Pollen-based quantitative climate reconstructions suggest that annual precipitation in this wettest period (6.2 to 5.1 cal kaBP) was greater than 550 mm (Xu et al., 2010), broadly consistent with the precipitation reconstruction from the carbon isotope ratio of black carbon (Wang et al., 2013b). Additionally, the large-scale expansion of Daihai Lake at ~7.3–3.2 cal kaBP (Sun et al., 2009) implies intensified monsoonal rainfall and a more humid climate in the lake basin, coincident with the geochemical record from a sediment core (Xiao et al., 2006). However, some proxy records show a longer wet interval, extending back to the early Holocene. In the Anguli Nuur region, on the basis of multi-proxy paleoclimatic reconstructions, Wang et al. (2010) defined the wettest interval of 8.9–7.4 cal kaBP as the Holocene optimum; furthermore, Yin et al. (2011) proposed a humidity time series based on a sediment grain size sequence and reported a generally humid climate ranging from 10.4 to 7.0 kaBP. A quantitative climate reconstruction from pollen and algal data in Bayanchagan Lake emphasized that the wettest climate occurred between 10.5 and 6.5 cal kaBP, at which time annual precipitation was up to 30%–60% higher than present

* Corresponding author. E-mail: tianfei@cags.ac.cn

(Jiang et al., 2006; 2010). High-resolution mineral magnetic and pollen records from Xiari Nuur, in the southern part of the Otindag sandy land, also show climatic improvement after ca. 11.7 cal kaBP with the most humid conditions prevailing until ~8.5 cal kaBP (Tang et al., 2015); the oxygen isotope content of authigenic carbonate reached a minimum at 8.3 kaBP, indicating a strong summer monsoon (Sun et al., 2018).A multi-proxy record reconstructed from the Haolaihure Paleolake section, located in the southeastern Otindag sandy land, reveals a relatively warm and wet stage from 8.7 to 2.2 cal kaBP (Liu et al., 2018). The Holocene optimum registered in the lacustrine sequence from Chagan Nuur has been characterized by the dominance of open forest steppe in the lake basin during 8.88–6.27 cal kaBP (Niu, 2018).

Conflicting views of Holocene monsoonal rainfall have developed from palaeoclimatic reconstructions of the same lake. On basis of the OSL chronology, and sedimentological and granulometric analysis, Zhang et al. (2011; 2012) reported that lake levels of Huangqihai were relatively stable and high in the early Holocene (> 8 kaBP); lake shrinkage due to persistent drought commenced at 8.7 kaBP, which contradicts the pollen record (Hao et al., 2014). The lake level history of Dali Lake reconstructed from multi-proxy analyses of a sediment core (Xiao et al., 2008; Fan et al., 2017; 2018) and from radiocarbon and OSL dating of lake beach ridges and sediment outcrops (Goldsmith et al., 2017), shows high-stands during the early and middle Holocene (11.5–5.9 cal kaBP). Xiao et al. (2008) attributed high lake levels in the early Holocene to the input of snow/ice melt from the Great Khingan Mountains, and lake expansion during the middle Holocene can be correlated to the strengthening monsoonal precipitation. However, Goldsmith et al. (2017) attributed high lake levels in the early Holocene to an increase in annual rainfall, signifying the northward migration of the EASM. It is noteworthy that the high-resolution pollen record from Dali Lake contradicts the view that the monsoonal rainfall increased during the early Holocene, and instead indicates that the EASM intensified after ~8.0 cal kaBP in northern China (Wen et al., 2017). Pollen-assemblage data from Hulun Lake demonstrate the expansion of grasses and birch forests from 8.0 to 6.4 cal kaBP, implying a remarkable increase in monsoonal precipitation (Wen et al., 2010a; 2010b); however, the past hydrological conditions deduced from species assemblages and the shell chemistry of ostracods show that high-stands of Hulun Lake were sustained from 11.6 to 6.2 cal kaBP (Zhai et al., 2011). Based on the above discussion, the sensitivity of temperate steppe to Holocene monsoonal precipitation has been assessed. As fossil pollen in lacustrine sediments provides direct information on variations in the composition and pattern of regional vegetation, we use pollen and spore data of a sediment core from Huangqihai Lake to reconstruct Holocene vegetation and climate changes. We firstly clarified Holocene climate change in the Huangqihai Lake region based on our pollen record and prior paleoclimatic reconstructions, and then conducted regional comparisons between our data and pollen records from other lakes in the steppe region to explore the regional evolution of vegetation, climate and associated EASM variations during the Holocene.

2 Geological Settings

Huangqihai Lake (40°41'–41°43'N, 112°49'–113°40'E, elevation 1268 m) is located in central Inner Mongolia, close to the northern boundary of the EASM (Fig. 1a, b). The area of the Huangqihai Lake is about 110 km^2, and its catchment area is ~4510 km^2 (Zhang et al., 2011; 2012). The average water depth is about 2.0 m, with a maximum depth of ~10 m. As a brackish water lake, the salinity of Huangqihai Lake is 11‰–12‰ and the mineralization degree is 7–7.2 g/L; the lake water is moderately alkaline, with an average pH of 9.3 (Peng, 2014).

According to meteorological data (1980–2010) from Jining weather station (station code: 53480), the mean annual temperature and precipitation are 4.7°C and 343.8 mm, respectively; nearly 70% of the precipitation falls in the summer months (JJA) and is associated with the moisture-carrying summer monsoon (Liu et al., 2018). The most frequent wind direction is W–NWN with a mean wind speed of 2.5 m/s. As a hydrologically closed lake, about 19 rivers (including Bawang River, Quanyulin River) enter the lake but there is no outflow. However, most of these rivers have been intermittent or even dry over the past decades as a result of human activities and climatic deterioration.

For the forest-steppe ecotone in northern China, the zonal vegetation pattern is steppe with forest patches and the azonal vegetation includes swamp, halophytic vegetation, and meadows around lakes (Peng, 2014). In the catchment area of Huangqihai Lake, steppe is the dominant vegetation type, with occasional forest patches. On the surrounding mountains, the main tree taxa include *Pinus tabulaeformis*, *Picea meyeri*, *Populus davidiana*, *Betula phatyphylla*, *Ulmus pumila* and *Salix* spp. (Hao et al., 2014). *Stipa krylovii* is the constructive species in steppe and other herbs in the communities include *Leymus chinensis*, *Artemisia frigida*, *Thalictrum aquilegiifolium*, *Cleistogenes squarrosa* etc. Halophytic meadow around the lake is characterised by an abundance of *Achnatherum splendens* (Hou, 2001). Additionally, there is scattered farmland in the study area, which primarily grow maize and wheat.

3 Methods

We recovered a 970-cm long sediment core (HQ; 40°48′ 23.00″, 113°17′49.80″) from Huangqihai Lake in 2007 using a piston corer (Fig. 1c). The uppermost 40 cm has been separated at a 1-cm resolution, and analysed for ^{210}Pb and ^{137}Cs at the Institute of Geology and Geophysics, Chinese Academy of Sciences. The ^{137}Cs-corrected constant rate of supply (CRS) model was used to calculate ^{210}Pb ages. Five accelerator mass spectrometry (AMS) radiocarbon dates on bulk organic matter were measured in the AMS Laboratory of Peking University. An age-depth model was established in R (The R Core Team, 2015) using the Bacon package (Blaauw and Christen, 2011), and the IntCal13 curve (Reimer et al., 2013) was used for radiocarbon calibration.

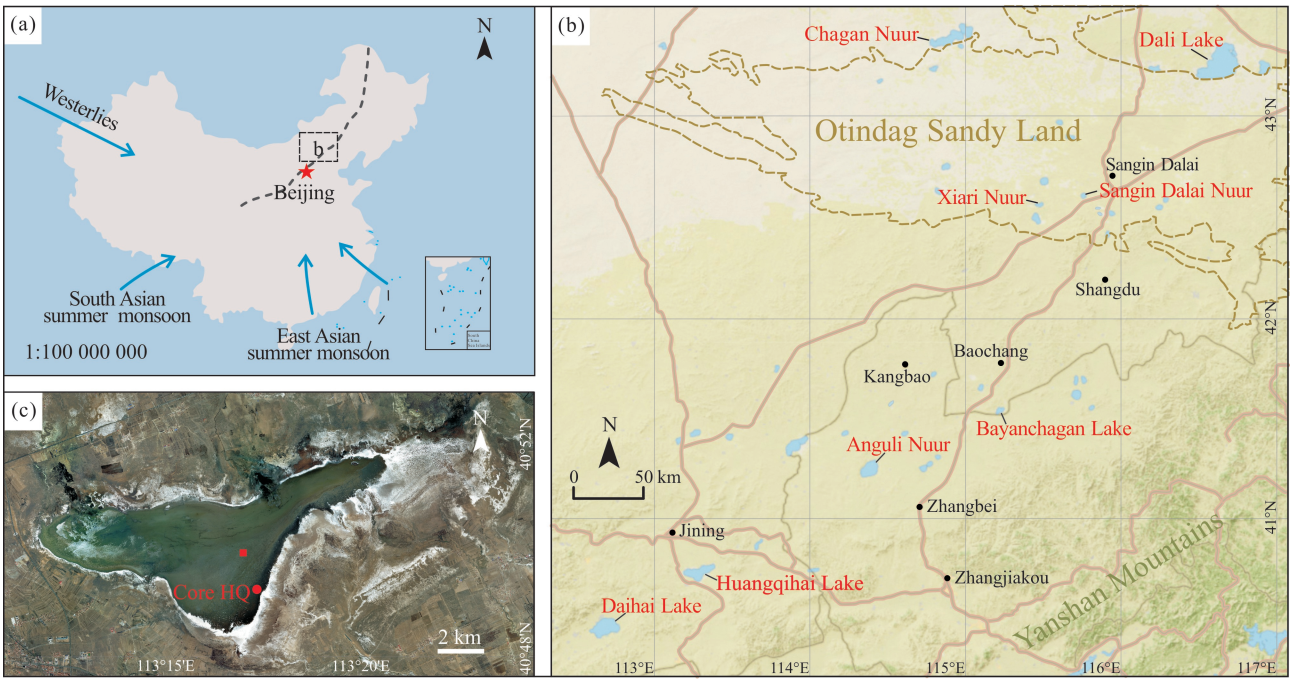

Fig. 1. Location of Huangqihai Lake within China (a) and Inner Mongolia (b), and the remote sensing image showing the location of core HQ (c). Note that China basemap is after China National Bureau of Surveying and Mapping Geographical Information and the grey dash line represents the location of EASM northern boundary according to Chen et al. (2018); the red square shows the location of coring site from Hao et al. (2014).

A total of 103 samples were collected for pollen analysis. Pollen taxa were identified in the Institute of Hydrogeology and Environmental Geology, Chinese Academy of Geological Science. Samples were pretreated on the basis of the HCl–NaOH–HF method described by Fægri et al. (1989). For better extraction and enrichment of pollen grains, samples were subjected to heavy liquid separation. A known quantity of *Lycopodium* spores was added prior to acidification to calculate the pollen concentration. Pollen grains were identified and counted using a light microscope (Olympus BX51) at ×400 magnification. About 400 pollen grains were counted for each sample. Pollen diagrams were plotted using Tilia (Grimm, 1991), and pollen assemblage zones were defined by stratigraphically-constrained cluster analysis using the sum of squares analysis (CONISS). Pollen taxa with percentages >5% in at least two samples were selected for ordination analysis in R using the Vegan package (Oksanen et al., 2017). Detrended correspondence analysis (DCA) showed a maximum axis length of 1.81, indicating a likely linear response of the pollen assemblages to environmental variables (Braak et al., 1988) and ensuring the application of principal components analysis (PCA). In addition, pollen-based proxies, including the *Artemisia* to Chenopodiaceae (A/C) pollen ratios and arboreal to non-arboreal (AP/NAP) pollen ratios, were calculated to assist with interpretation of the results.

4 Results

4.1 Lithology and chronology

Core HQ is composed mainly of yellow to yellowish-brown silt, intercalated with several sandy silt layers (Fig. 2). Notably, a 20-cm-thick grey-brown clayey silt layer is present at the middle of the core. The grain sizes of sediments become coarser at the bottom, and yellow and grey-white sandy silt layers occur at 760–816 cm and 900–970 cm, respectively. Chronological control for core HQ is provided by AMS ^{14}C and ^{210}Pb ages (Table 1, Fig. 2a). We consider ^{137}Cs as a reliable chronomarker, and the highest value at 13.5 cm was linked to the peak fallout of ^{137}Cs in 1963 CE (Fig. 2b). $^{210}Pb_{ex}$ activities follow an exponentially declining trend with depth (Fig. 2b). Hence, we apply the ^{137}Cs-corrected CRS model to core HQ. The carbon reservoir was estimated by the age difference between our ^{210}Pb age and the AMS ^{14}C age from Hao et al. (2014) at the depth of 3 cm. Due to the generally linear growth in age with depth throughout the core, we assumed a constant reservoir age of 1587 yr. According to the Bacon age-depth model, the basal age of core HQ is 10.7 cal kaBP. The deposition rate of the upper 40 cm is about 0.21 cm/yr, and decreases downwards to 0.09 cm/yr.

4.2 Pollen assemblage zones

Ninety-six pollen and spore taxa were identified in core HQ. The pollen and spore assemblages are dominated by herbaceous taxa, with an average pollen percentage of 59.9%, composed of *Artemisia*, Chenopodiaceae, Gramineae, Ranunculaceae, Leguminosae, Polygonaceae, etc. The arboreal taxa consist of *Pinus*, *Quercus*, *Betula*, *Carpinus*, *Juglan*, *Alnus*, *Ulmus*, Cupressaceae, *Tilia* etc., with an average pollen percentage of 27.6%. The shrub pollen and fern spores in core HQ are quite rare, with

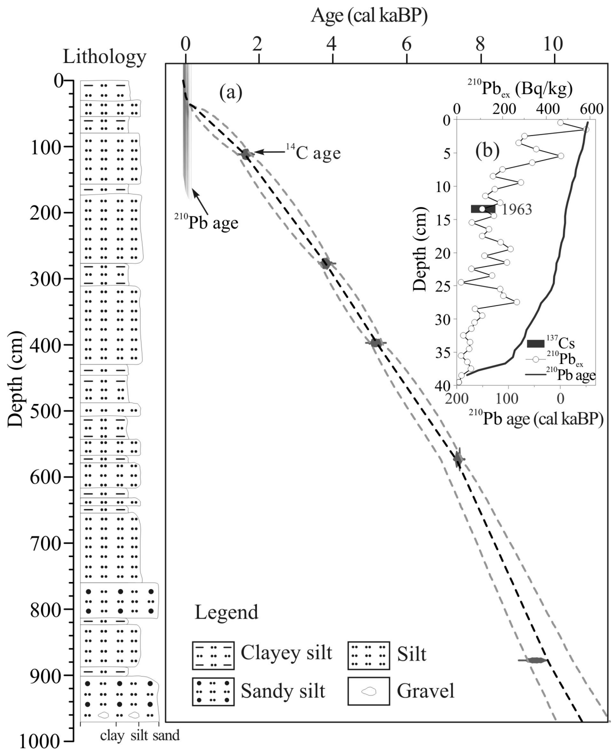

Fig. 2. Lithology and bacon age model (a) incorporating ^{210}Pb ages and calibrated, reservoir corrected ^{14}C ages for core HQ; the grey stippled lines show 95% confidence intervals, and the black curve shows the single 'best' model. The inset (b) shows unsupported ^{210}Pb ($^{210}Pb_{ex}$) activities and calculated ^{210}Pb ages versus depth for the uppermost 40 cm of core HQ.

Table 1 AMS radiocarbon dates of samples from core HQ

Sample No.	Depth (cm)	Dating material	^{14}C age (^{14}C yr BP)
HQ-UP-2	112	Bulk organic matter	3320±45
HQ-UP-3	277	Bulk organic matter	5120±35
HQ-UP-4	397	Bulk organic matter	6095±30
HQ-2-①	573	Bulk organic matter	8075±30
HQ-3	877	Bulk organic matter	9850±100

pollen percentages of 3.4% and 1.2% on average. Common taxa include *Ephedra*, *Nitraria*, *Adiantum*, *Sellaginella Sinensis*, *Athyrium*, and Filicale. Pollen and spore percentages of selected taxa are presented in Fig. 3 and the pollen spectra are divided into four pollen assemblage zones (PAZs) as follows:

4.2.1 PAZ 1 (957–754 cm, 10.7–8.8 cal kaBP)

In zone 1, the pollen spectra show an absolute dominance of herbaceous pollen, which contribute up to 70.0%. After an initial increase to 42.3%, Chenopodiaceae pollen declines to 7.9%, while *Artemisia* pollen is relatively abundant (40.1%). Other common herbaceous taxa including Gramineae, Compositae (*Chrysanthemum*, *Taraxacum* and *Aster*), Ranunculaceae (mainly *Thalictrum*) and Cyperaceae occurred at low frequencies. Arboreal pollen mainly derived from *Pinus* (2.5%–32.1%) accounts for 7.8%–45.7% of the pollen sum, while shrub pollen, represented by *Hippophae*, *Ephedra* and *Nitraria*, is present at low frequencies (3.1%). Fern spores were noted, and the Filicale spores, identified in most samples, reach a percentage of 2.8%.

4.2.2 PAZ 2 (754–562 cm, 8.8–7.2 cal kaBP)

In zone 2, arboreal pollen fluctuated between 6.3% and 87.8%. The predominant pollen contributor, *Pinus*, increased to 81.2% around 8.4 cal kaBP and then sharply decreased. Shrub pollen maintains relatively low frequencies, but a slight increasing trend in *Ephedra* (up to 8.2%) was noticed. The proportion of herbaceous taxa decreases to an average of 54.2%, much lower than that in the preceding zone. Both Gramineae and Chenopodiaceae pollen displays low and stable percentages, while *Artemisia* pollen fluctuates to a considerable extent, ranging from 4.9% to 82.7%. The fern spores, with the major contribution from Filicale, are consistently low in the proportion.

4.2.3 PAZ 3 (562–233 cm, 7.2–3.2 cal kaBP)

The pollen assemblages of zone 3 are characterized by a considerable increase in arboreal pollen, with a high average percentage of 57.9%. *Pinus* pollen contributes 20.7%–86.4% of the total pollen sum and reaches the highest average percentage (52.1%) within core HQ. Broadleaved tree taxa including *Betula*, *Carpinus*, *Quercus* and *Ulmus* showed obvious decreases after 5.3 cal kaBP. Shrub pollen remains at low percentages (3.1%) and *Hippophae* is absent. Herbaceous pollen decreases to its lowest average percentage (36.9%) and the dominant taxa, such as Gramineae (3.6%), Chenopodiaceae (10.3%) and *Artemisia* (17%), also display low percentages when compared with other zones. Fern spores, especially *Adiantum*, *Athyrium* and Filicale, increased slightly after 5.3 cal kaBP.

4.2.4 PAZ 4 (233–0 cm, <3.2 cal kaBP)

The pollen assemblages of zone 4 are marked by a dramatic decrease in arboreal pollen (17.4%). *Pinus* pollen decrease to an average percentage of 13.8, and other tree taxa, including *Picea*, *Abies*, *Betula*, *Carpinus* etc., are present at low frequencies (< 2%). Despite averages of shrub pollen from zones 3 and 4, a decreasing trend in *Ephedra* and increasing trend in *Nitraria* were noted. Increases in the proportions of Gramineae (12.9%), Chenopodiaceae (24.9%) and *Artemisia* (34.4%) lead to the dominance of herbaceous pollen (79%) in this zone. Moreover, *Taraxacum* and *Primula* pollen reached their peaks in core HQ. It is noteworthy that the percentages of spores are extremely low, and *Athyrium* is virtually absent in this zone.

4.3 PCA results

PCA ordination of the main terrestrial pollen taxa from core HQ provides a visual representation of the main trends in the pollen data and reflects the pattern of local terrestrial vegetation development (Fig. 4). The first two PCA axes capture 22.8% and 18.0% of the total variance within the pollen data set. The eigenvectors for the selected pollen taxa are plotted in Fig. 4, and the lengths of the arrows roughly correspond to their relative contributions to the variance. PC1 is positively correlated with *Betula*, *Quercus*, *Pinus*, *Ephedra*, and *Ranuncula*, and negatively correlated with Chenopodiaceae,

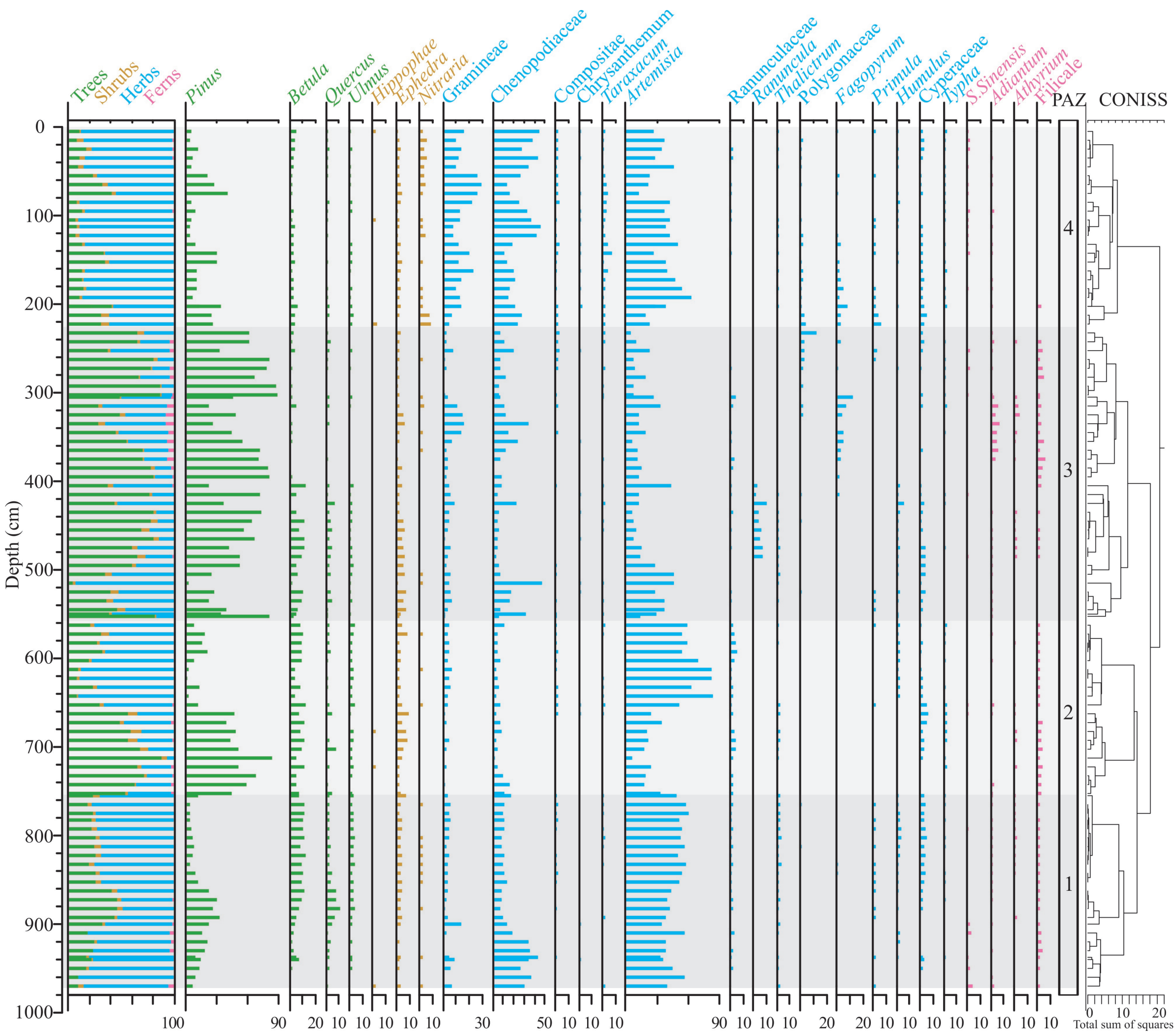

Fig. 3. Percentage pollen diagram for core HQ.

Gramineae, *Nitraria*, Polygonaceae, etc. Hence, high values of PC1 may represent a shift of vegetation type to forest steppe, whereas a decrease in PC1 may be linked with vegetation degradation to typical steppe or even desert steppe. As shown by the scatter diagram, the samples from PAZ 1 are distributed in the first and second quadrants, and samples from PAZ 2 occur mainly in the first and fourth quadrants. Samples from PAZ 3 are dispersed in the third and fourth quadrants, while samples from PAZ 4 are primarily concentrated in the second quadrant.

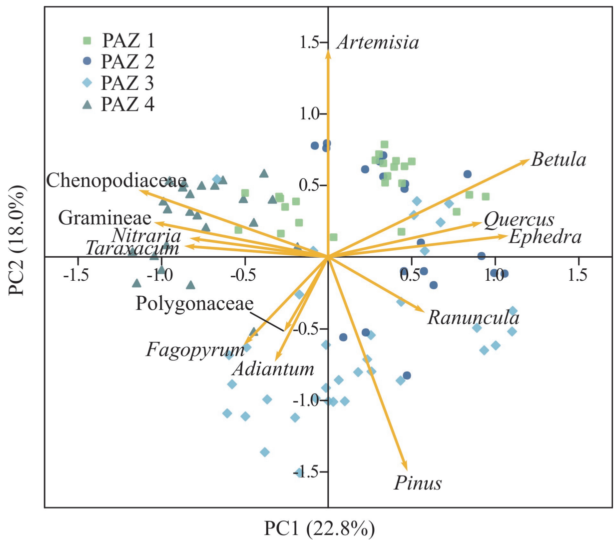

Fig. 4. PCA ordination of selected taxa with percentages > 5% in at least two samples and the total pollen data of core HQ.

5 Discussion

5.1 Holocene vegetation and climate change in the Huangqihai Lake region

During 10.7–8.8 cal kaBP, the pollen assemblages were characterized by high percentages of herbaceous (mainly *Artemisia*) pollen, together with low A/C pollen ratios, indicating that typical steppe was dominant around the lake area. Small forest patches only appeared in a short interval (10–9.7 cal kaBP), as indicated by the high tree pollen percentages (>30%) (Xu et al., 2007) and the AP/NAP ratios (Liu et al., 1999; Huang et al., 2019). Obvious increases in tree pollen and AP/NAP ratios have been interpreted as the expansion of forest at 8.8–8.0 cal kaBP; this forest may have comprised pine, oak and elm due to the under-representation of *Quercus* and *Ulmus* pollen (Xu et al., 2007). Hence, a moderately wet climate prevailed in the Huangqihai Lake region during the early Holocene, shifting to wetter conditions until 8.0 cal kaBP as deduced by the expansion of forest. Multi-proxy reconstructions of a section in the drainage basin revealed enhanced weathering, implying warm and arid conditions from 10.6 to 7.8 cal kaBP (Hao et al., 2010). There is a general consensus regarding the stepwise increase in lake level during the early Holocene; however, whether or not the maximum Holocene lake-level was attained in the early Holocene is still controversial (Zhang et al., 2011; Xu et al., 2012).

During 8.0 to 7.2 cal kaBP, a transition to steppe has been indicated by the predominance of *Artemisia* and rapidly increasing A/C pollen ratios. The dominance of steppe in another pollen record, at 8.6–7.2 cal kaBP, (Hao et al., 2014) commenced earlier than in our record. The extremely dry subinterval ranged from 8.0 to 7.6 cal kaBP was also evidenced by the retreat of Huangqihai Lake (Zhang et al., 2011). Subsequently, the abundance of tree pollen and high AP/NAP imply that a forest steppe landscape dominated the lake area from 7.2 to 3.2 cal kaBP, consistent with the pollen record from Hao et al. (2014). The humid conditions in the middle Holocene are supported by geochemical analysis (Hao, 2010). Moreover, the absence of broadleaved trees after 5.2 cal kaBP and the stepwise decline of PC1 together indicate a gradual drying trend. The signal of climatic deterioration has also been seized in the hydrological records, as the lake level began to decline after 6.7 cal kaBP (Zhang et al., 2011; Xu, 2012), superposed on centennial-scale fluctuations in lake level (Wang et al., 2010). The dry climate after ~5.0 kaBP led to the collapse of a short-lived period of habitation (5.5–5 kaBP) in the Huangqihai Lake region (Mo et al., 2003). Additionally, relatively low values of tree pollen, AP/NAP and PC1 from 4.5 to 4.1 cal kaBP indicate a centennial-scale climate deterioration, which might be linked to the 4.2 ka event.

After 3.2 cal kaBP the herbaceous taxa, including Gramineae, Chenopodiaceae and *Artemisia*, significantly increased, suggesting a transition to steppe around the lake. Meanwhile, tree cover declined to its lowest levels (Mo et al., 2003). Chenopodiaceae plants in salty meadows grew on saline and alkaline soil near the water, and contributed strongly to pollen in the lake sediments (Han et al., 2017). The retreat of Huangqihai Lake led to the development of halophytic meadow dominated by Chenopodiaceae (mainly *Achnatherum splendens*). Hence, extremely low A/C values associated with the abundance of Chenopodiaceae pollen imply a dryer climate than before (Wang et al., 2020), consistent with reduced chemical weathering in the catchment (Hao, 2010). As a result of persistent drought, Huangqihai Lake was turned into a playa after 2.2 cal kaBP (Zhang et al., 2011).

5.2 Spatial patterns of vegetation and climate at the northwestern fringe of the EASM

Precipitation has been considered as the most important limiting factor for vegetation development in the forest-steppe ecotone of northern China (Liu et al., 2006; Li et al., 2011). Hence, changes in pollen assemblages in response to precipitation can be used to interpret variations in monsoon intensity (Zhao and Yu, 2012). Pollen records (Fig. 5) from the lakes located at the northwestern fringe of the EASM, quantified by percentages of tree or *Pinus* pollen and pollen-based moisture indexes, have been selected to compile the spatial patterns of vegetation and climate and explore the EASM variations. During the early Holocene (>8 cal kaBP), landscape comprising steppe with small patches of forest dominated the lake regions of Huangqihai, Dali (Wen et al., 2017), Daihai (Xiao et al., 2004) and Hulun (Wen et al., 2010a) as shown by the relatively low tree pollen percentages, indicating a relatively dry climate. The increasing trends in *Pinus* pollen from the Anguli Nuur area (Liu et al., 2010) and Bayanchagan Lake (Jiang et al., 2006) revealed stepwise increasing humidity in the early Holocene. Moreover, except for the quantitative climate reconstructions from Daihai Lake (Xu et al., 2010), we consider that the mean annual precipitation in the Hulun Lake area (Wen et al., 2010b), the moisture indexes for the Bayanchagan Lake area (Jiang et al., 2010) and even the temperate steppe region (Zhao et al., 2009) indicate that the climate was not drier than present, and instead was moderately wet in the early Holocene.

The middle Holocene (8–4 cal kaBP) was characterized by high percentages of tree pollen, suggesting the expansion of forest in the Huangqihai Lake region. The expansion of forest has also been reported in the areas around Dali Lake (Wen et al., 2017), Daihai Lake (Xiao et al., 2004) and Hulun Lake (Wen et al., 2010a). Enhanced precipitation during the middle Holocene has been widely reported in the quantitative climate reconstructions from Daihai Lake (Xu et al., 2010), Hulun Lake (Wen et al., 2010b) and in the synthesized moisture indexes (Zhao et al., 2009; Liu et al., 2010), suggesting the northward movement of the EASM. In addition, climate drying since ~5 ka has been detected in the pollen records from Huangqihai Lake and Anguli Nuur, coincident with the declining moisture indexes.

After ~4 cal kaBP, declining forest and a shift to steppe were detected by all pollen records, indicating a persistent dry climate prevailing in the temperate steppe region, and suggesting reduced monsoon intensity. Our record shows that steppe dominated the Huangqihai Lake region after 3.2 cal kaBP, which is earlier than the period indicated by the pollen record from Daihai Lake (Xiao et al., 2004). In Anguli Nuur, the long-term replacement of the forest zone by steppe commenced at 2.1 kaBP (Liu et al., 2010). The discrepancies in the onset and duration of forest recession are attributed to the influence of topography, as altitudinal migration of trees in areas with a large altitude range may prevent or buffer forest disappearance when the climate is not suitable (Hao et al., 2016; Cheng et al., 2018).

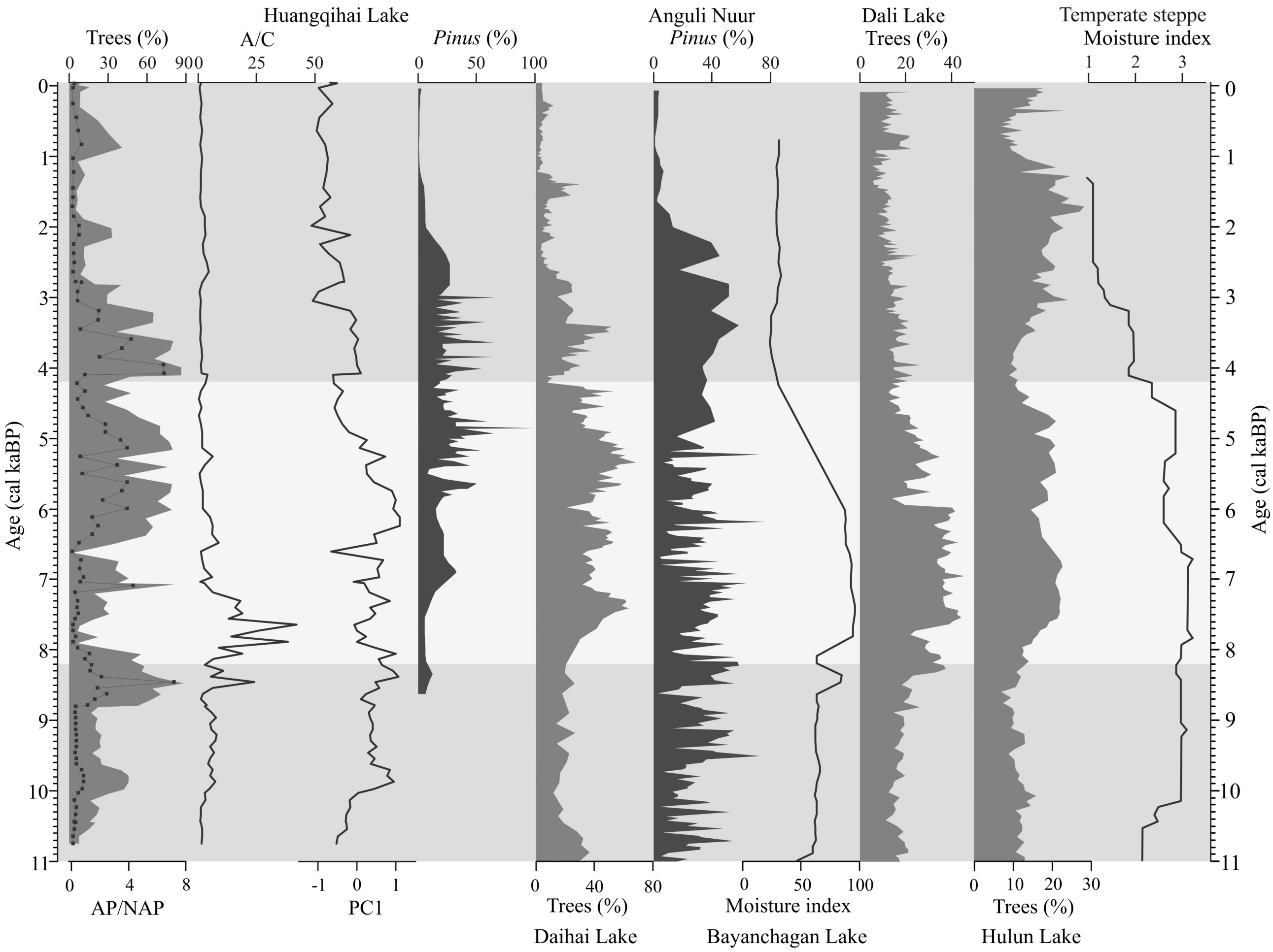

Fig. 5. Tree pollen percentages, AP/NAP pollen ratios, A/C pollen ratios and PC1 values from our study, tree pollen percentages from Daihai Lake (Xiao et al., 2004), *Pinus* pollen percentages from Anguli Nuur (Liu et al., 2010), pollen-based moisture index from Bayanchagan Lake (Jiang et al., 2010), tree pollen percentages from Dali Lake (Wen et al., 2017), Hulun Lake (Wen et al., 2010a), and synthesized moisture index (Zhao et al., 2009).

6 Conclusions

Pollen analysis of a sediment core extracted from Huangqihai Lake provide a continuous record of Holocene vegetation and climate changes. The pollen assemblages suggest that typical steppe with small forest patches dominated the lake area from 10.7 to 8.8 cal kaBP, as indicated by high percentages of herbaceous pollen (especially *Artemisia* and Chenopodiaceae), suggesting moderately wet conditions. The following short interval of 8.8–8.0 cal kaBP was characterized by increasing tree pollen percentages; this expansion of forest reflects an amelioration of climatic conditions. During 8.0 to 7.2 cal kaBP, a transition to steppe was revealed by the predominance of *Artemisia*, highlighting a centennial-scale dry event (8.0–7.6 cal kaBP). A generally humid climate prevailed in the lake area from 7.2 to 3.2 cal kaBP, as indicated by the abundance of tree pollen and the high AP/NAP. Moreover, the absence of broadleaved trees and the stepwise decrease of PC1 together indicate general drying after 5.2 cal kaBP. The centennial-scale climate deterioration from 4.5 to 4.1 cal kaBP is considered to be a response to the 4.2 ka event. After 3.2 cal kaBP, herbaceous taxa including Gramineae, Chenopodiaceae and *Artemisia* all significantly increased, suggesting a transition to steppe under severe drought conditions, consistent with pollen contributions from halophytic meadow around the lake. Our results are broadly comparable with other paleoclimate records from the Huangqihai Lake region, and indicate that climate was moderately wet in the early Holocene (10.7–7.2 cal kaBP), wettest in the middle Holocene (7.2–3.2 cal kaBP), and dry in the late Holocene (after 3.2 cal kaBP). The pollen records from lakes located in the temperate steppe region show complex patterns of vegetation evolution and associated climate change; nevertheless, forest showed a clear expansion in the middle Holocene, corresponding to the enhanced EASM.

Acknowledgements

This work was funded by the Geological Survey Projects of China (Grant Nos. DD20190370 and DD20190009). This work was also supported by Natural Science Foundation of

Shaanxi Province, China (Grant No. 2019JQ-835), Research Foundation of Education Bureau of Shaanxi Province, China (Grant No. 2019JK-0404). We thank the reviewers for their thorough comments and suggestions that help clarify and improve the paper.

Manuscript received Apr. 5, 2020
accepted Jun. 5, 2020
associate EIC: DING Xiaozhong
edited by FEI Hongcai

References

Blaauw, M., and Christen, J.A., 2011. Flexible paleoclimate age-depth models using an autoregressive gamma process. Bayesian Analysis, 6(3): 457–474.

Braak, C.J.F.T., Prentice, C., and Ter Braak, C.J.F., 1988. A theory of gradient analysis. Advances in Ecological Research, 18: 271–317.

Chen, J., Huang, W., Jin, L.Y., Chen, J., Chen, S.Q., and Chen, F.H., 2018. A climatological northern boundary index for the east Asian summer monsoon and its interannual variability. Science China Earth Sciences, 61(1): 13–22.

Cheng, Y., Liu, H.Y., Wang H.Y., and Hao Q., 2018. Differentiated climate-driven Holocene biome migration in western and eastern China as mediated by topography. Earth-Science Reviews, 182: 174–185.

Fægri, K., Kaland, P.E., and Krzywinski, K., 1989. Textbook of Pollen Analysis 4th Edition. New York: John Wiley & Sons, 1–328.

Fan, J.W., Xiao, J.L., Wen, R.L., Zhang, S.R., Huang, Y., Yue, J.J., Wang, X., Cui, L.L., Li, H., Xue, D.S., and Liu, Y.H., 2018. Mineralogy and carbonate geochemistry of the Dali Lake sediments: Implications for paleohydrological changes in the East Asian summer monsoon margin during the Holocene. Quaternary International, 479: 148–159.

Fan, J.W., Xiao, J.L., Wen, R.L., Zhang, S.R., Wang, X., Cui, L.L., and Yamagata, H., 2017. Carbon and nitrogen signatures of sedimentary organic matter from Dali Lake in Inner Mongolia: Implications for Holocene hydrological and ecological variations in the East Asian summer monsoon margin. Quaternary International, 452: 65–78.

Goldsmith, Y., Broecker, W.S., Xu, H., Polissar, P.J., Demenocal, P.B., Porat, N., Lan, J.H., Cheng, P., Zhou, W.J., and An, Z.S., 2017. Northward extent of East Asian monsoon covaries with intensity on orbital and millennial timescales. Proceedings of the National Academy of Sciences, 114(8): 1817–1821.

Grimm, E.C., 1991. TILIA and TILIAGRAPH software. Springfield: Illinois State Museum.

Guo, L.C., Xiong, S.F., Ding, Z.L., Jin, G.Y., Wu, J.B., and Ye, W., 2018. Role of the mid-Holocene environmental transition in the decline of late Neolithic cultures in the deserts of NE China. Quaternary Science Reviews, 190: 98–113.

Han, Y., Liu, H.Y., Hao, Q., Liu, X., Guo, W.C., and Shangguan, H., 2017. More reliable pollen productivity estimates and relative source area of pollen in a forest-steppe ecotone with improved vegetation survey. The Holocene, 27(10): 1567–1577.

Hao, C., Wang, Y., and Yao, P.Y., 2010. Middle-late Holocene environmental changes recorded by lacustrine sediments from Huangqihai Lake, Inner Mongolia. Bulletin of Mineralogy, Petrology and Geochemistry, 2(29): 149–156 (In Chinese with English abstract).

Hao, Q., Liu, H.Y., Yin, Y., Wang, H.Y., and Feng, M.M., 2014. Varied responses of forest at its distribution margin to Holocene monsoon development in northern China. Palaeogeography, Palaeoclimatology, Palaeoecology, 409: 239–248.

Hao, Q., Liu, H.Y., and Liu, X.Y., 2016. Pollen-detected altitudinal migration of forests during the holocene in the mountainous forest–steppe ecotone in northern China. Palaeogeography, Palaeoclimatology, Palaeoecology, 446: 70–77

Hou, X.Y., 2001. The Vegetation Atlas of China (1:1000 000). Beijing: Science Press, 1–280 (In Chinese).

Huang, M., Li, M.C., Fan, H.Y., Zhang, X.F., Li, J.J., and Xu, Q.M., 2019. Late Cenozoic climate and sedimentary environment evolution of the northwestern coast of the Bohai Bay revealed by borehole QHJ01. Acta Geologica Sinica, 93 (4): 899–914 (in Chinese with English abstract).

Jiang, W.Y., Guiot, J., Chu, G.Q., Wu, H.B., Yuan, B.Y., Hatté C., and Guo Z.T., 2010. An improved methodology of the modern analogues technique for palaeoclimate reconstruction in arid and semi-arid regions. Boreas, 39(1): 145–153.

Jiang, W.Y., Guo, Z.T., Sun, X.J., Wu, H.B., Chu, G.Q., Yuan, B.Y., Hatté, C., and Guiot, J., 2006. Reconstruction of climate and vegetation changes of Lake Bayanchagan (Inner Mongolia): Holocene variability of the East Asian monsoon. Quaternary Research, 65: 411–420.

Li, X.Q., Zhou, J., Shen, J., Weng, C.Y., Zhao, H.L., and Sun, Q.L., 2004. Vegetation history and climatic variations during the last 14 ka BP inferred from a pollen record at Daihai Lake, north-central China. Review of Palaeobotany and Palynology, 132(3–4): 195–205.

Li, Y.C., Bunting, M.J., Xu, Q.H., Jiang, S.X., Ding, W., and Hun, L.Y., 2011. Pollen-vegetation-climate relationships in some desert and desert-steppe communities in northern China. The Holocene, 21(6): 997–1010.

Liu, H.Y., Cui, H.T., Pott, R., and Speier, M., 1999. The surface pollen of the woodland-steppe ecotone in southeastern Inner Mongolia, China. Review of Palaeobotany and Palynology, 105(3): 237–250.

Liu, H.Y., Wang, Y., Tian, Y.H., Zhu, J.L., and Wang, H.Y., 2006. Climatic and anthropogenic control of surface pollen assemblages in East Asian steppes. Review of Palaeobotany and Palynology, 138(3–4): 281–289.

Liu, H.Y., Yin, Y., Zhu, J.L., Zhao, F.J., and Wang, H.Y., 2010. How did the forest respond to Holocene climate drying at the forest–steppe ecotone in northern China? Quaternary International, 227: 46–52.

Liu, J., Wang, Y., Wang, Y., Guan, Y.Y., Dong, J., and Li, T.D., 2018. A multi-proxy record of environmental changes during the Holocene from the Haolaihure Paleolake sediments, Inner Mongolia. Quaternary International, 479: 148–159.

Liu, S.S., Liu, D.B., Wang, Y.J., and Zhao, K., 2018. Asian hydroclimate changes and mechanisms in the preboreal from an annually-laminated stalagmite, Daoguan Cave, southern China. Acta Geologica Sinica (English Edition), 92(1): 367–377.

Mo, D.W., Wang, H., and Li, S.C., 2003. Effects of Holocene environmental changes on the development of archaeological cultures in different regions of North China. Quaternary Sciences 23(2): 200–210 (In Chinese with English abstract).

Niu, Z.M., 2018. Vegetation and climate changes during the Holocene reflected by lacustrine records (Master Thesis). Hohhot: Hohhot University, 1–79.

Oksanen, J., Blanchet, F.G., Kindt, R., Legendre, P., Minchin, P., O Hara, R.B., Simpson G., Solymos P., Stevens M., and Wagner H., 2017. Vegan: community ecology package. R package vegan, vers. 2.4-2.

Peng, X.M., 2014. Paleohydrologic reconstruction of special Holocene stages in Lake Huang Qihai in Inner Mongolia, China (Master Thesis). Nanchang: Jiangxi Normal University, 1–46.

Reimer, P.J., Bard, E., Bayliss, A., Beck, J.W., Blackwell, P.G., Ramsey, C.B., Buck, C.E., Cheng, H., Edwards, R.L., Friedrich, M., Grootes, P.M., Guilderson, T.P., Haflidason, H., Hajdas, I., Christine, H., Heaton, T.J., Hoffmann, D.L., Hogg, A.G., Hughen, K.A., Kaise, K.F., Kromer, B., Manning, S.W., Niu, M., Reimer, R.W., Richards, D.A., Scott, E.M., Southon, J.R., Staff, R.A., Turney, C.S.M., and van der Plicht, J., 2013. IntCal13 and marine13 radiocarbon age calibration curves 0–50,000 years Cal BP. Radiocarbon, 55(4): 1869–1887.

Sun, Q., Chu, G.Q., Xie, M.M., Zhu, Q.Z., Su, Y.L., and Wang, X.S., 2018. An oxygen isotope record from Lake Xiarinur in Inner Mongolia since the last deglaciation and its implication for tropical monsoon change. Global and Planetary Change, 163: 109–117.

Sun, Q.L., Wang, S.M., Zhou, J., Shen, J., Cheng, P., Xie, X.P., and Wu, F., 2009. Lake surface fluctuations since the late glaciation at Lake Daihai, North central China: A direct indicator of hydrological process response to East Asian monsoon climate. Quaternary International, 194: 45–54.
Tang, L., Wang, X.S., Zhang, S.Q., Chu, G.Q., Chen, Y., Pei, J.L., Sheng, M., and Yang, Z.Y., 2015. High-resolution magnetic and palynological records of the last deglaciation and Holocene from Lake Xiarinur in the Hunshandake Sandy Land, Inner Mongolia. The Holocene, 25(5): 844–856.
The R Core Team, 2015. R: a language and environment for statistical computing. R Foundation for Statistical Computing, Vienna: 1–3405.
Wang, H., Liu, H., Zhu, J., and Yin, Y., 2010. Holocene environmental changes as recorded by mineral magnetism of sediments from Anguli-nuur Lake, southeastern Inner Mongolia Plateau, China. Palaeogeography, Palaeoclimatology, Palaeoecology, 285(1–2): 30–49.
Wang, H.Y., Liu, H.Y., Cui, H.T., and Abrahamsen, N., 2001. Terminal Pleistocene/Holocene palaeoenvironmental changes revealed by mineral-magnetism measurements of lake sediments for Dali Nor area, southeastern Inner Mongolia Plateau, China. Palaeogeography, Palaeoclimatology, Palaeoecology, 170: 115–132.
Wang, X., Cui, L.L., Xiao, J.L., and Ding, Z.L., 2013b. Stable carbon isotope of black carbon in lake sediments as an indicator of terrestrial environmental changes: An evaluation on paleorecord from Daihai Lake, Inner Mongolia, China. Chemical Geology, 347: 123–134.
Wang, X., Xiao, J.L., Cui, L.L., and Ding, Z.L., 2013a. Holocene changes in fire frequency in the Daihai Lake region (north-central China): indications and implications for an important role of human activity. Quaternary Science Reviews, 59: 18–29.
Wang, Y., Wang, W., Liu, L., Jiang, Y.J., Niu, Z.M., Ma, Y.Z., He, J., and Mensing, S.A., 2020. Reliability of theArtemisia/ Chenopodiaceae pollen ratio in differentiating vegetation and reflecting moisture in arid and semi-arid China. The Holocene: 095968362090221.
Wang, Y., Yao, P.Y., Chi, Z.Q., Guan, Y.Y., and Zhao, Z.L., 2010. Middle-Late Holocene environmental changes recorded by lacustrine sediments from Huangqihai Lake, Inner Mongolia. Bulletin of Mineralogy, Petrology and Geochemistry, 29(2): 149–156 (In Chinese with English abstract).
Wen, R.L., Xiao, J., Chang, Z.G., Zhai, D.Y., Xu, Q.H., Li, Y.C., and Itoh, S., 2010b. Holocene precipitation and temperature variations in the East Asian monsoonal margin from pollen data from Hulun Lake in northeastern Inner Mongolia, China. Boreas, 39: 262–272.
Wen, R.L., Xiao, J.L., Chang, Z.G., Zhai, D.Y., Xu, Q.H., Li, Y.C., Itoh, S., and Lomtatidze, Z., 2010a. Holocene climate changes in the mid-high-latitude-monsoon margin reflected by the pollen record from Hulun Lake, northeastern Inner Mongolia. Quaternary Research, 73: 293–303.
Wen, R.L., Xiao, J.L., Fan, J.W., Zhang, S.R., and Yamagata, H., 2017. Pollen evidence for a mid-Holocene East Asian summer monsoon maximum in northern China. Quaternary Science Reviews, 176: 29–35.
Xiao, J.L., Chang, Z.G., Fan, J.W., Zhou, L., Zhai, D., Wen, R.L., and Qin, X.G., 2012. The link between grain-size components and depositional processes in a modern clastic lake. Sedimentology, 59(3): 1050–1062.
Xiao, J.L., Chang, Z.G., We,n R.L., Zhai, D.Y., Itoh, S., and Lomtatidze, Z., 2009. Holocene weak monsoon intervals indicated by low lake levels at Hulun Lake in the monsoonal margin region of northeastern Inner Mongolia, China. The Holocene, 19(6): 899–908.
Xiao, J.L., Si, B., Zhai, D.Y., Itoh, S., and Lomtatidze, Z., 2008. Hydrology of Dali Lake in central-eastern Inner Mongolia and Holocene East Asian monsoon variability. Journal of Paleolimnology, 40: 519–528.
Xiao, J.L., Wu, J.T., Si, B., Liang, W.D., Nakamura, T., Liu, B.L., and Inouchi, Y., 2006. Holocene climate changes in the monsoon/arid transition reflected by carbon concentration in Daihai Lake of Inner Mongolia. The Holocene, 16: 551–560.
Xiao, J.L., and Xu, Q.H., Nakamura, T., Yang, X.L., Liang, W.D., and Inouchi, Y., 2004. Holocene vegetation variation in the Daihai Lake region of north-central China: a direct indication of the Asian monsoon climatic history. Quaternary Science Reviews, 23(14–15): 1669–1679.
Xu, J.J., Jia, Y.L., Lai, Z.P., Wang, P.L., Xu, M., and Shen, H.Y., 2012. Climate variations during early to mid-Holocene in Huangqihai Lake in northern China based on the lake deposit analysis. Acta Sedimentologica Sinica, 30(4): 731–738 (In Chinese with English abstract).
Xu, Q.H., Li,, Y.C., Yang, X.L., and Zheng, Z.H., 2007. Quantitative relationship between pollen and vegetation in northern China. Science in China Series D: Earth Sciences, 50 (4): 582–599.
Xu, Q.H., Xiao, J.L., Li, Y.C., Tian, F., and Nakagawa, T., 2010. Pollen-based quantitative reconstruction of Holocene climate changes in the Daihai Lake area, Inner Mongolia, China. Journal of Climate, 23: 2856–2868.
Yang, S.L., Dong, X.X., and Xiao, J.L., 2018. The East Asian Monsoon since the Last Glacial Maximum: Evidence from geological records in northern China. Science China Earth Sciences: 2–12.
Yin, Y., Liu, H.Y., He, S.Y., Zhao, F.J., Zhu, J.L., Wang, H.Y., Liu, G., and Wu, X.C., 2011. Patterns of local and regional grain size distribution and their application to Holocene climate reconstruction in semi-arid Inner Mongolia, China. Palaeogeography, Palaeoclimatology, Palaeoecology, 307: 168 –176.
Zhai, D.Y., Xiao, J.L., Zhou, L., Wen, R.L., Chang, Z.G., Wang, X., Jin, X.D., Pang, Q.Q., and Itoh, S., 2011. Holocene East Asian monsoon variation inferred from species assemblage and shell chemistry of the ostracodes from Hulun Lake, Inner Mongolia. Quaternary Research, 75(3): 512–522.
Zhang, J.R., Jia, Y.L., Lai, Z.P., Long, H., and Yang, L.H., 2011. Holocene evolution of Huangqihai Lake in semi-arid northern China based on sedimentology and luminescence dating. The Holocene, 21(8): 1261–1268.
Zhang, J.R., Lai, Z.P., and Jia, Y.L., 2012. Luminescence chronology for late Quaternary lake levels of enclosed Huangqihai lake in East Asian monsoon marginal area in northern China. Quaternary Geochronology, 10: 123–128.
Zhao, Y., and Yu, Z.C., 2012. Vegetation response to Holocene climate change in East Asian monsoon-margin region. Earth-Science Reviews, 113: 1–10.
Zhao, Y., Yu, Z.C., Chen, F.H., Zhang, J.W., and Yang, B., 2009. Vegetation response to Holocene climate change in monsoon-influenced region of China. Earth-Science Reviews, 97: 242–256.

About the first and corresponding author

TIAN Fei, female, born in 1985 in Tai'an City, Shandong Province; doctor; graduated from China University of Geosciences (Beijing); research assistant of the Institute of Geology, Chinese Academy of Geological Sciences. She is now interested in the study on late Quaternary lacustrine deposits and paleoclimatic reconstructions. Email: tianfei@cags.ac.cn; phone: 15120086529.